*Inorg. Chem.* **2005**, *44*, 4979–4982


# $Sr_2MnSb_2$: A New Ternary Transition Metal Zintl Phase

**Seon-Mi Park,[†] Sung-Jin Kim,*[,†] and Mercouri G. Kanatzidis*[,‡]**

*Department of Chemistry, Ewha Womans University, Seoul, Korea 120-750, and Department of Chemistry and Center for Fundamental Materials Research, Michigan State University, East Lansing, Michigan 48824*

Received December 12, 2004

A transition metal-containing Zintl phase, $Sr_2MnSb_2$, was prepared from a stoichiometric combination reaction of the elements in Sn flux, and its structure was determined by single-crystal X-ray diffraction methods. The compound crystallizes in the orthorhombic space group *Pnma* with $a = 15.936(3)$ Å, $b = 14.498(3)$ Å, $c = 8.2646(17)$ Å, and $Z = 12$. The structure of $Sr_2MnSb_2$ is composed of corrugated layers of corner- and edge-shared $MnSb_4$ tetrahedra. The basic building unit of the layer is a $[Mn_3Sb_6]^{12-}$ cluster composed of three edge-shared $MnSb_4$ tetrahedra. These trinuclear clusters share four Sb vertexes to form a layer with cavities. $Sr^{2+}$ cations are located at the inter- and intralayer space. Magnetic susceptibility measurements indicate an effective magnetic moment of 4.85 $\mu_B$, a value smaller than what would be expected from $Mn^{2+}$ ions.

## Introduction

Although there is a large number of ternary main group Zintl phases, there are relatively few with transition metals.[1] Interest in ternary manganese pnictides derives from the novel anionic frameworks and unusual magnetic properties that can be observed from the interactions among the partially filled d orbitals of manganese. $AMn_2Sb_2$ (A = Ca, Sr, Ba, Eu, Yb) crystallizes as either the $CaAl_2Si_2$-type (A = Ca, Sr, Eu, Yb)[2] or the $ThCr_2Si_2$-type (A = Ba).[3] Isostructural analogues such as $SrMn_2P_2$ and $EuMn_2P_2$ exhibit antiferromagnetic transitions because of the high-spin $d^5$ $Mn^{2+}$ cations.[4] The $A_{14}MnSb_{11}$ family of compounds (A = Ca, Sr, Ba, Eu, Yb) has been studied extensively and was shown to possess interesting magnetic behavior and GMR (giant magnetoresistance) or CMR (colossal magnetoresistance) properties.[5,6] One formula unit of $A_{14}MnSb_{11}$ consists of 14 $A^{2+}$ cations, 4 $Sb^{3-}$ monomers, a $[MnSb_4]^{9-}$ tetrahedron, and a linear anion, $Sb_3^{-}$.[7] $Sr_{14}MnSb_{11}$ has ferromagnetic properties, and the Mn cations have been claimed to be trivalent with a high-spin $d^4$ state.[6g] $RE_6MnSb_{15}$ (RE = La, Ce) has a nonclassical Sb sublattice network, a three-dimensional $Sb_{20}$, a one-dimensional $Sb_3$ strip, and

* To whom correspondence should be addressed. E-mail: kanatzid@cem.msu.edu. Phone: +1 517-353-0174 (M.G.K.). E-mail: sjkim@ewha.ac.kr. Phone: +82 2-3277-2350 (S.-J.K.).

† Ewha Womans University.

‡ Michigan State University.

(1) (a) Gascoin, F.; Sevov, S. C. *Inorg. Chem.* **2003**, *42*, 8567. (b) Gascoin, F.; Sevov, S. C. *Inorg. Chem.* **2003**, *42*, 904. (c) Gascoin, F.; Sevov, S. C. *Inorg. Chem.* **2002**, *41*, 5920. (d) Gascoin, F.; Sevov, S. C. *Inorg. Chem.* **2002**, *41*, 2820. (e) Huang, D.; Corbett, J. D. *Inorg. Chem.* **1998**, *37*, 4006. (f) Kauzlarich, S. M., Ed. *Chemistry, Structure, and Bonding of Zintl Phases and Ions*; VCH Publishers: New York, 1996. (g) Holm, A. P.; Olmstead, M. M.; Kauzlarich, S. M. *Inorg. Chem.* **2003**, *42*, 1973. (h) Kim, H.; Condron, C. L.; Holm, A. P.; Kauzlarich, S. M. *J. Am. Chem. Soc.* **2000**, *122*, 10720. (i) Bobev, S.; Thompson, J. D.; Sarrao, J. L.; Olmstead, M. M.; Hope, H.; Kauzlarich, S. M. *Inorg. Chem.* **2004**, *43*, 5044. (j) Sologub, O.; Vybornov, P.; Rogl, P.; Hiebl, K.; Cordier, G.; Woll, P. *J. Solid State Chem.* **1996**, *122*, 266. (k) Kim, H.; Condron, C. L.; Holm, A. P.; Kauzlarich, S. M. *J. Am. Chem. Soc.* **2000**, *122*, 10720. (l) Holm, A. P.; Park, S.-M.; Condron, C. L.; Kim, H.; Klavins, P.; Grandjean, F.; Hermann, R. P.; Long, G. J.; Kanatzidis, M. G.; Kauzlarich, S. M.; Kim, S.-J. *Inorg. Chem.* **2003**, *42*, 4660. (m) Park, S.-M.; Kim, S.-J. *J. Solid State Chem.* **2004**, *177*, 3418. (n) Macaluso, R. T.; Wells, D. M.; Sykora, R. E.; Albrecht-Schmitt, T. E.; Mar, A.; Nakatsuji, S.; Lee, H.; Fisk, Z.; Chan, Julia Y. *J. Solid State Chem.* **2004**, *177*, 293. (o) Raju, N. P.; Greedan, J. E.; Ferguson, M. J.; Mar, A. *Chem. Mater.* **1998**, *10*, 3630. (p) Ferguson, M. J.; Hushagen, R. W.; Mar, A. *J. Alloys Compds.* **1997**, *249*, 191.

(2) (a) Cordier, G.; Schäfer, H. *Z. Naturforsch.* **1976**, *31*, 1459. (b) Rühl, R.; Jeitschko, W. *Mater. Res. Bull.* **1979**, *14*, 513.

(3) Brechtel, E.; Cordier, G.; Schäfer, H. *Z. Naturforsch.* **1979**, *34*, 921.

(4) (a) Brock, S. L.; Greedan, J. E.; Kauzlarich, S. M. *J. Solid State Chem.* **1994**, *109*, 416. (b) Brock, S. L.; Greedan, J. E.; Kauzlarich, S. M. *J. Solid State Chem.* **1994**, *113*, 303. (c) Payne, A. C.; Sprauve, A. E.; Olmstead, M. M.; Kauzlarich, S. M. *J. Solid State Chem.* **2002**, *163*, 498.

(5) Cordier, G.; Schäfer, H.; Stelter, M. *Z. Anorg. Allg. Chem.* **1984**, *519*, 183.

(6) (a) Chan, J. Y.; Kauzlarich, S. M.; Klavins, P.; Shelton, R. N.; Webb, D. J. *Chem. Mater.* **1997**, *9*, 3132−3135. (b) Chan, J. Y.; Wang, M. E.; Rehr, A.; Kauzlarich, S. M.; Webb, D. J. *Chem. Mater.* **1997**, *9*, 2131. (c) Chan, J. Y.; Olmstead, M. M.; Kauzlarich, S. M.; Webb, D. J. *Chem. Mater.* **1998**, *10*, 3583. (d) Kim, H.; Chan, J. Y.; Olmstead, M. M. *Chem. Mater.* **2002**, *14*, 206. (e) Kim, H.; Klavins, P.; Kauzlarich, S. M. *Chem. Mater.* **2002**, *14*, 2308. (f) Rehr, A.; Kauzlarich, S. M. *J. Alloys Compds.* **1994**, *207*, 424. (g) Rehr, A.; Kuromoto, T. Y.; Kauzlarich, S. M.; Castillo, J. D.; Webb, D. J. *Chem. Mater.* **1994**, *6*, 93.

10.1021/ic048252e CCC: $30.25 
Published on Web 06/09/2005

isolated $Sb^{3-}$ species. The magnetic susceptibility data of $RE_6MnSb_{15}$ indicate that the rare earth elements are trivalent and that Mn is divalent.[1j] $Sr_{21}Mn_4Sb_{18}$ showed a single anionic framework consisting of $Sb^{3-}$ monomers, $Sb_2^{4-}$ dimers, and $[Mn_8Sb_{22}]^{48-}$ isolated tetrahedral clusters.[1k] The recently reported $Eu_{10}Mn_6Sb_{13}$ has a distinctive structure formed by a condensation of "$MnSb_4$" tetrahedra. The anionic framework of $Eu_{10}Mn_6Sb_{13}$ is assembled with edge- and corner-sharing of the Mn-centered tetrahedra forming cavities. These cavities are occupied by $[Sb_2]^{4-}$ dumbbells and $Eu^{2+}$ cations, where all of the Mn atoms are divalent.[1l]

Our ongoing efforts to prepare new Zintl compounds[1l,m,7] with transition metals resulted in the discovery of $Sr_2MnSb_2$ which features a unique two-dimensional corrugated anionic framework. Here, we report the synthesis, crystal structure, and magnetic properties of $Sr_2MnSb_2$.

## Experimental Section

**Synthesis.** $Sr_2MnSb_2$ was synthesized from the elements Sr (Aldrich, chips, 99.9%), Mn (Aldrich, powder, 99.9%), and Sb (high purity, powder, 99.999%) using the Sn (Junsei, drops, 99.9%) flux method. All manipulations were performed in a $N_2$-filled glovebox. The mixture of elements (Sr/Mn/Sb/Sn = 10:6:13:30) was placed into a graphite tube which was then vacuum sealed inside of a silica tube. The mixture was heated to 1000 °C at a rate of 10 °C/h, held at 1000 °C for 24 h, cooled to 550 °C at 5 °C/h, held at 550 °C for 4 days, and then cooled to room temperature at 5 °C/h. After reaction, the excess Sn flux was removed from the product as follows. $SiO_2$ wool was inserted into the tube and rested over the graphite tube that contained product. Then the silica tube was again evacuated and sealed. The tube was inverted, placed in a box furnace and heated to 500 °C at a rate of 100 °C/h and kept at that temperature for 2 h, after which the tube was transferred quickly from the furnace to a centrifuge and spun immediately. The excess Sn flux passed through the $SiO_2$ wool and gathered in the bottom of the tube, leaving an abundance of black chuck single crystals of $Sr_2MnSb_2$ behind. Interestingly, when we attempted to synthesize this compound without Sn flux, we obtained $SrMn_2Sb_2$ as the majority phase. The sample $Sr_2MnSb_2$ is sensitive to moist air and must be handled under an inert atmosphere.

**Electron Microscopy.** Semiquantitative microprobe analysis of the compounds was performed with a JEOL JSM-35C scanning electron microscope (SEM) equipped with a Tracor Northern energy dispersive spectroscopy (EDS) detector. Data were acquired using an accelerating voltage of 20 kV and a 30 s accumulation time. Semiquantitative microprobe analysis on single crystals gave the formula $Sr_{1.5(2)}Mn_{1.0(2)}Sb_{1.9(2)}$ (average of three data acquisitions). The slightly lower Sr content (1.52 vs 2.0) is a symptom of the EDS technique which is only semiquantitative. The refinement of the X-ray data does not support a deficiency of Sr on its site as its occupancy refined to a 100%.

**Table 1.** Selected Data from the Single-Crystal Structure Refinement of $Sr_2MnSb_2$

| | |
|---|---|
| empirical formula | $Sr_2MnSb_2$ |
| fw | 473.68 |
| temp (K) | 173(2) |
| wavelength ($\lambda = K_\alpha$, Å) | 0.71073 |
| cryst syst | orthorhombic |
| space group | *Pnma* (No. 62) |
| unit cell dimensions (Å) | $a = 15.946(3)$ |
| | $b = 14.498(3)$ |
| | $c = 8.2646(17)$ |
| vol (Å$^3$) | 1910.7(7) |
| $Z$ | 12 |
| $\rho_{calc}$ (g/cm$^3$) | 4.940 |
| absorption coefficient (mm$^{-1}$) | 26.792 |
| reflns collected/unique | 11288/2222 |
| data/restraints/parameters | 2222/0/77 |
| final R indices [$F_o^2 > 2\sigma(F_o^2)$][a] | $R_1 = 0.0290$, $wR_2 = 0.0568$ |
| R indices ($F_o^2 > 0$) | $R_1 = 0.0422$, $wR_2 = 0.0595$ |
| largest diff. peak and hole (e/Å$^3$) | 1.567 and −1.222 |

[a] $R_1 = [\sum|F_o| - |F_c|]/\sum|F_o|$ and $wR_2 = \{[\sum w[(F_o)^2 - (F_c)^2]^2]/[\sum w(F_o^2)^2]\}^{1/2}$ for $F_o^2 > 2\sigma(F_o^2)$ and $w = [\sigma^2(F_o)^2 + (0.0342P)^2]^{-1}$ where $P = (F_o^2 + 2F_c^2)/3$.

**Magnetic Property.** Magnetic susceptibility measurements for $Sr_2MnSb_2$ were performed using a MPMS quantum designed SQUID magnetometer. The measurements on the crystal samples were done under increasing temperature (5−300 K) with a 5000 G applied field.

**Crystallographic Studies.** A black crystal with dimensions of 0.01 × 0.01 × 0.004 mm was mounted on a glass fiber at 173 K. A Bruker AXS SMART Platform CCD diffractometer equipped with a low-temperature apparatus was used to collect intensity data using graphite monochromatized Mo Kα radiation. The data set was collected over a half sphere of reciprocal space up to 56° in $2\theta$ at 173.1(2) K. The individual frames were measured with a $\omega$ rotation of 0.3° and an acquisition time of 45 s. The initial 50 frames of data were measured again at the end of the data collection procedure and compared to the initial readings to check the stability of the crystal. No crystal decay was detected. The SMART software was used for data acquisition, and SAINT was used for data extraction and reduction.[8] The absorption correction was performed empirically using SADABS.[9] With the low-temperature data, the unit cell parameters were obtained from least-squares refinements using 600 randomly chosen reflections from a full sphere of reciprocal space up to 56° in $2\theta$, see Table 1. The observed Laue symmetry and systematic extinctions were indicative of the space groups *Pnma* and $Pn2_1a$. The centrosymmetric space group *Pnma* was chosen, and the subsequent refinements confirmed the choice of this space group. The initial positions of all of the atoms were obtained from direct methods, and the structure was refined by full-matrix least-squares techniques with the use of the SHELXL-97 program package.[9] Once all of the atoms were located, the occupancies of the successive atoms were allowed to vary, but the refinements did not lead to any significant change in the occupation factor. The final cycle of refinement performed on $F_o^2$ with 77 variables and 2222 averaged reflections converged to residual $wR_2$ ($F_o^2 > 0$) = 0.0595. The conventional R index based on reflections having $F_o^2 > 2\sigma(F_o^2)$ was 0.0290. The final difference Fourier synthesis map showed maximum and minimum peaks of 1.567 and −1.222 e/Å$^3$, respectively. The complete data collection parameters and details of the structure solution and refinement for two different

(7) (a) Kim, S.-J.; Hu, S. Q.; Uher, C.; Kanatzidis, M. G. *Chem. Mater*. **1999**, *11*, 3154. (b) Kim, S.-J.; Hu, S. Q.; Uher, C.; Hogan, T.; Huang, B. Q.; Corbett, J. D.; Kanatzidis, M. G. *J. Solid State Chem*. **2000**, *153*, 321. (c) Kim, S.-J.; Ireland, J.; Kannewurf, C. R.; Kanatzidis, M. G. *Chem. Mater*. **2000**, *12*, 3133. (d) Kim, S.-J.; Ireland, J.; Kannewurf, C. R.; Kanatzidis, M. G. *J. Solid State Chem*. **2000**, *155*, 55. (e) Kim, S.-J.; Kanatzidis, M. G. *Inorg. Chem.* **2001**, *40*, 3781. (f) Kim, S.-J.; Salvador, J.; Bilc, D.; Mahanti, S. D.; Kanatzidis, M. G. *J. Am. Chem. Soc*. **2001**, *123*, 12704. (g) Park, S.-M.; Choi, E. S.; Kang, W.; Kim, S.-J. *J. Mater. Chem.* **2002**, *12*, 1839. (h) Park, S.-M.; Kim, S.-J.; Kanatzidis, M. G. *J. Solid State Chem*. **2003**, *175*, 310. (i) Park, S.-M.; Kim, S.-J.; Kanatzidis, M. G. *J. Solid State Chem*. **2004**, *177*, 2867.

(8) *SMART* and *SAINT*, version 5; Siemens Analytical X-ray System, Inc.: Madison, WI, 1998.

(9) Sheldrick, G. M. *SADABS*; University of Göttingen: Göttingen, Germany, 1998.

**Table 2.** Atomic Coordinates ($\times 10^4$) and Equivalent Isotropic Displacement Parameters ($\times 10^3$ Å$^2$) for $Sr_2MnSb_2$

| atom | Wyckoff position | *x* | *y* | *z* | *U*(eq)[a] |
|---|---|---|---|---|---|
| Sr(1) | 4c | 6274(1) | 7500 | 9100(1) | 9(1) |
| Sr(2) | 8d | 6138(1) | 5988(1) | 4127(1) | 8(1) |
| Sr(3) | 8d | 3910(1) | 5593(1) | 1265(1) | 8(1) |
| Sr(4) | 4c | 3757(1) | 7500 | 5027(1) | 7(1) |
| Sb(1) | 4c | 4988(1) | 7500 | 2074(1) | 6(1) |
| Sb(2) | 8d | 4755(1) | 5959(1) | 7409(1) | 6(1) |
| Sb(3) | 4c | 7505(1) | 7500 | 5827(1) | 7(1) |
| Sb(4) | 8d | 7487(1) | 5704(1) | 680(1) | 6(1) |
| Mn(1) | 8d | 2966(1) | 5877(1) | 7588(1) | 7(1) |
| Mn(2) | 4c | 4218(1) | 7500 | 9040(1) | 7(1) |

[a] *U*(eq) is defined as $^1/_3$ of the trace of the orthogonalized $U_{ij}$ tensor.

**Table 3.** Selected Bond Distances (Å) and Angles (deg) in $Sr_2MnSb_2$

| | | | |
|---|---|---|---|
| Mn(1)−Sb(2) | 2.8584(13) | Mn(2)−Sb(1) | 2.7922(17) |
| Mn(1)−Sb(3) | 2.7920(12) | Mn(2)−Sb(2) ×2 | 2.7456(11) |
| Mn(1)−Sb(4) | 2.7969(12) | Mn(2)−Sb(3) | 2.7340(17) |
| Mn(1)−Sb(4) | 2.8177(13) | | |
| Sr(1)−Sb(1) | 3.2006(12) | Sr(3)−Sb(1) | 3.3236(9) |
| Sr(1)−Sb(2) ×2 | 3.5791(10) | Sr(3)−Sb(2) | 3.2861(9) |
| Sr(1)−Sb(3) | 3.3419(13) | Sr(3)−Sb(2) | 3.5005(10) |
| Sr(1)−Sb(4) ×2 | 3.4970(9) | Sr(3)−Sb(4) | 3.3285(9) |
| Sr(2)−Sb(1) | 3.3235(1) | Sr(3)−Sb(4) | 3.3989(9) |
| Sr(2)−Sb(2) | 3.4071(10) | Sr(4)−Sb(1) | 3.1317(12) |
| Sr(2)−Sb(2) | 3.4959(10) | Sr(4)−Sb(2) ×2 | 3.3759(9) |
| Sr(2)−Sb(3) | 4.3057(12) | Sr(4)−Sb(4) ×2 | 3.3509(9) |
| Sr(2)−Sb(4) | 3.5320(9) | Mn(1)−Mn(2) | 3.311(2) |
| Sr(2)−Sb(4) | 3.5939(10) | Mn(1)−Mn(1) | 5.074(2) |
| Sb(3)−Mn(1)−Sb(4) | 112.48(4) | Sb(3)−Mn(2)−Sb(2) | 109.34(4) |
| Sb(3)−Mn(1)−Sb(4) | 116.95(4) | Sb(2)−Mn(2)−Sb(2) | 108.89(6) |
| Sb(4)−Mn(1)−Sb(4) | 110.34(4) | Sb(3)−Mn(2)−Sb(1) | 113.79(6) |
| Sb(3)−Mn(1)−Sb(2) | 104.59(4) | Sb(2)−Mn(2)−Sb(1) | 107.68(4) |
| Sb(4)−Mn(1)−Sb(2) | 108.56(4) | Mn(1)−Sb(3)−Mn(1) | 114.89(5) |
| Sb(4)−Mn(1)−Sb(2) | 103.00(4) | Mn(1)−Sb(3)−Mn(2) | 73.61(3) |
| Sr(2)−Sr(1)−Sr(2) | 55.57(1) | Mn(1)−Sb(4)−Mn(1) | 129.32(3) |
| Sr(1)−Sr(2)−Sr(2) | 62.22(1) | Mn(1)−Mn(2)−Mn(1) | 90.59(3) |
| Sr(3)−Sr(4)−Sr(3) | 83.13(1) | | |
| Sr(4)−Sr(3)−Sr(3) | 48.44(1) | | |

temperatures are given in Table 1. Final atomic positions, isotropic thermal parameters, and selected bond distances are given in Tables 2 and 3.

## Results and Discussion

**Structural Description.** $Sr_2MnSb_2$ appears to have a new type of structure. The structure is composed of layers of $[MnSb_2]^{4-}$ with $Sr^{2+}$ cations separating the layers (Figure 1). Figure 2 shows a representation of the crystal structure down the *a* axis and a corrugated layer. The layers formed by the edge- and corner-sharing of Mn-centered tetrahedra have 12-membered rings and present well-defined grooves on both sides of their surface. The whole structure seems to be well packed with half of the $Sr^{2+}$ cations residing in the grooves and the rest between the corrugated layers. Figure 3 shows a fragment of $[MnSb_2]^{4-}$ anionic cluster layers and local Mn environments. The basic building unit of the layer is the $[Mn_3Sb_6]^{12-}$ cluster assembled from three edge-shared tetrahedra. These units are connected by sharing of four Sb atoms along the *bc* plane. In the basic building unit, a crystallographically imposed mirror plane perpendicular to the *b* direction runs through the Mn(2) site which is positioned on a 2/*m* symmetry site.

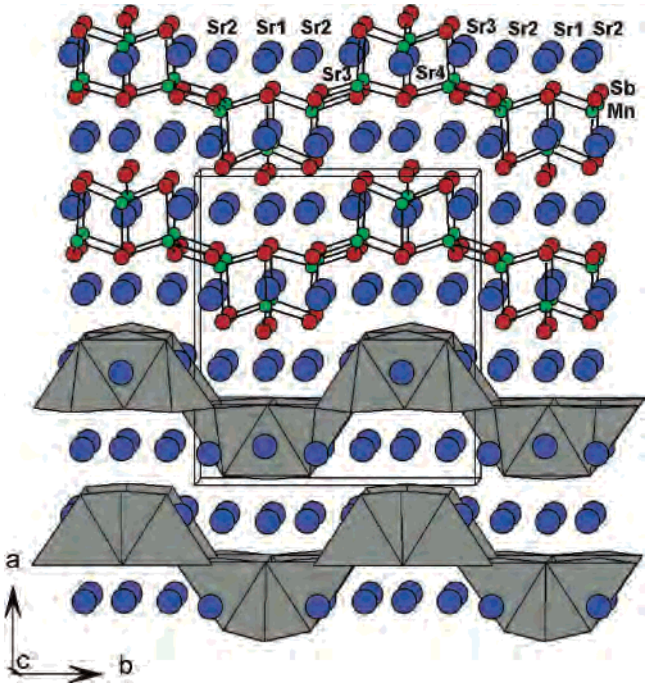


**Figure 1.** Representation of $Sr_2MnSb_2$ crystal structure down the *c* axis showing the unit cell outline. The Sr, Mn, and Sb atoms are indicated as blue, green, and red circles, respectively.

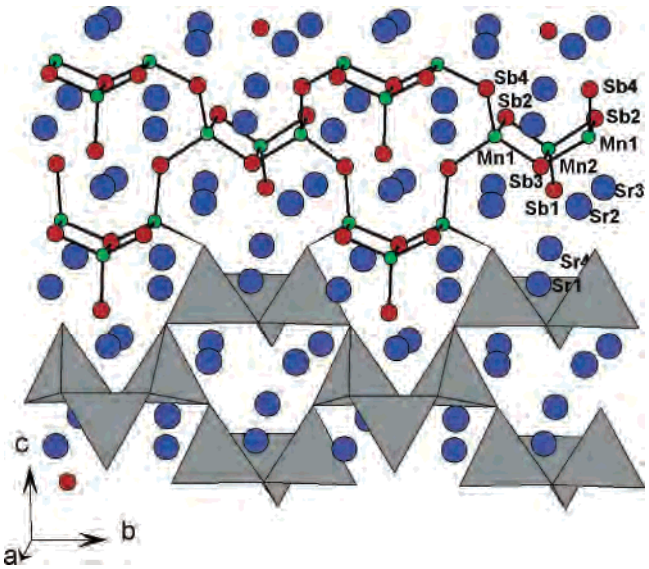


**Figure 2.** View down the *a* axis of the $Sr_2MnSb_2$. The Sr, Mn, and Sb atoms are indicated as blue, green, and red circles, respectively.

The anionic framework has four crystallographically different Sb atoms coordinated by two nonequivalent Mn atoms. Atoms Sb(2) and Sb(3) are shared by the Mn(1)- and Mn(2)-centered tetrahedra, forming the edge-shared basic building block. Sb(1) is a terminal atom coordinated only to Mn(2). The Sb(4) acts as a connector of two Mn atoms. The shortest Sb−Sb distance is 4.442(1) Å between Sb(2)−Sb(4).

The Mn−Sb bond lengths range from 2.7340(17) to 2.8584(13) Å. These bond distances are similar to those in $Sr_{21}Mn_4Sb_{18}$ (2.763−3.007 Å),[1k] $Sr_{14}MnSb_{11}$ (2.838 Å),[6g] $SrMn_2Sb_2$ (2.756−2.782 Å),[2a] and $Eu_{10}Mn_6Sb_{13}$ (2.679∼2.858 Å).[1l] The tetrahedral angles around the

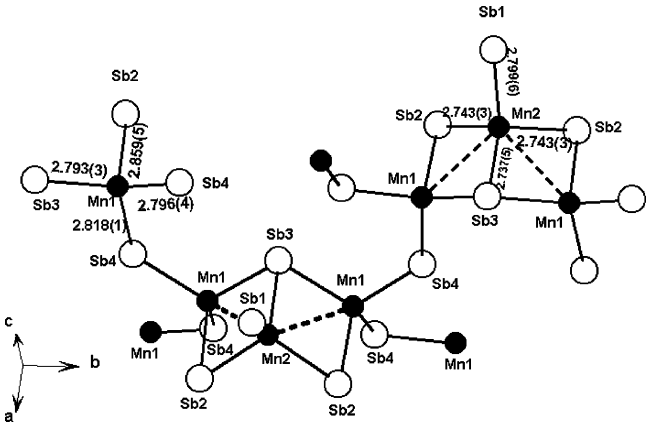


**Figure 3.** Fragment of a corrugated layer with atomic and bond distance (Å) labeling.

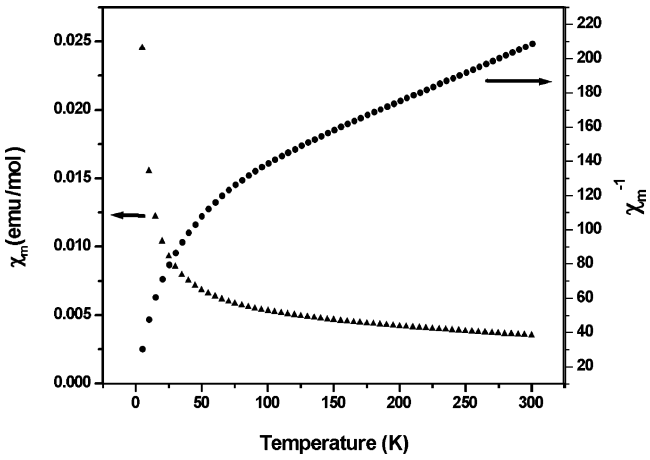


**Figure 4.** Magnetic susceptibility and inverse susceptibility as a function of temperature for $Sr_2MnSb_2$ at 5000 G.

Mn(1) and Mn(2) atoms range from 103.00(4) to 116.95(4)° and 108.89(6) to 113.79(6)°, respectively. The two Mn(1)- and Mn(2)-centered tetrahedra share two Sb(2)−Sb(3) edges to make a trimer with a Mn(1)−Mn(2) distance of 3.311(2) Å and a Mn(1)−Mn(2)−Mn(1) angle of 90.59(3)°. To our knowledge, this Mn trimer is unprecedented.

The $Sr_2MnSb_2$ structure has four crystallographically distinct Sr atoms. Sr(1) and Sr(2), placed in grooves of the corrugated layer, are surrounded by six Sb atoms with distorted octahedral geometries. Sr(3) and Sr(4) are surrounded by five Sb atoms with square pyramidal geometries and nested in grooves on the layer surfaces (Figure 1).

**Magnetic Properties.** Figure 4 shows the magnetic susceptibility and inverse susceptibility taken with an applied field of 5000 G. The overall shape of the magnetic susceptibility curve from 5 to 300 K indicates paramagnetic behavior. The inverse susceptibility above 100 K obeys the Curie−Weiss law with a Weiss temperature of −309.38 K, but below 100 K, a deviation from the Curie−Weiss law is observed. The rather large negative Weiss constant, Θ, suggests strong antiferromagnetic exchange interactions at low temperatures. The effective moment per formula unit of $Sr_2MnSb_2$ is 4.85 $\mu_B$. A free $Mn^{2+}$ ($d^5$) has an effective moment of 5.92 $\mu_B$ and that of $Mn^{3+}$ ($d^4$) is 4.90 $\mu_B$; therefore, the Mn atoms in $Sr_2MnSb_2$ could be considered to be trivalent. This would suggest that $Sr_2MnSb_2$ is a Zintl compound with an extra electron. However the valence assignment for $Mn^{2+}$ appears to be charge balanced as $(Sr^{2+})_2[Mn^{2+}(Sb^{3-})_2]^{4-}$. A recent report on $A_{14}MnSb_{11}$ (A = Ca, Yb) suggests that Mn is in a high-spin state, $d^5$, even though the experimental magnetic moment is more consistent with $Mn^{3+}$. This may be the result of a hole in the $Sb_4$ tetrahedron aligning parallel to the Mn moment.[10] A similar situation could be present in $Sr_2MnSb_2$. Bond valence sum calculations indicate a positive charge of 2.1 on Mn(1) and 2.5 on Mn(2).[11] We note that the existence of $Mn^{3+}$ ions in the presence of $Sb^{3-}$ species has never been documented. Arguably, the $Mn^{3+}/Sb^{3-}$ pair is not considered to be thermodynamically compatible given the high oxidizing power of $Mn^{3+}$ and the strong reducing character of $Sb^{3-}$.[12] This comes from the relative energy of the empty Mn d orbitals and the filled Sb p orbitals. The same situation exists in MnSb which is not a $Mn^{3+}$ compound.[13] A $Mn^{3+}$ configuration would place the energy of d orbitals below that of the filled Sb p orbitals. Therefore, a 3+ oxidation state for Mn is not expected to be stable in antimonides in particular and pnictides in general. Consequently, despite the lower than expected value of the magnetic moment in $Sr_2MnSb_2$, we still prefer a formal 2+ state for Mn.[14] Obviously, the mechanisms responsible for depressing the effective magnetic moment on the metal in $Sr_2MnSb_2$ and $Ca_{14}MnSb_{11}$ (they may or may not be the same in the two phases) need to be further investigated.

**Acknowledgment.** Financial support from the Department of Energy (Grant DE-FG02-99ER45793 to M.G.K.) is gratefully acknowledged. S.-J.K. acknowledges financial support from MOST of Korea. S.-M.P. was supported by the Postdoctoral Fellowship Program of the Korea Science & Engineering Foundation (KOSEF).

**Supporting Information Available:** Crystallographic information in CIF format. This material is available free of charge via the Internet at http://pubs.acs.org.

IC048252E

(10) (a) Holm, A. P.; Kauzlarich, S. M.; Morton, S. A.; Waddill, G. D.; Pickett, W. E.; Tobin, J. G. *J. Am. Chem. Soc.* **2002**, *124*, 9894. (b) Kim, H.; Hung, Q.; Lynn, J. W.; Kauzlarich, S. M. *J. Solid State Chem.* **2002**, *168*, 162.
(11) Brown, I. D.; Altermatt, D. *Acta Crystallogr. B* **1985**, *41*, 244.
(12) Sáchez-portal, D.; Martin, R. M.; Kauzlarich, S. M.; Pickett, W. E. *Phys. Rev. B* **2002**, *65*, 144414.
(13) (a) Endo K. *J. Phys. Soc. Jpn.* **1970**, *29*, 643. (b) Dewaard, H; Reintsem, S. R.; Pasterna, M. *Phys. Lett. B* **1970**, *33*, 413.
(14) Magnetic measurements were performed on a number of single crystals from different batches, repeatedly. A few crystals were chosen randomly from the sample for the magnetic measurement and were checked with a single-crystal X-ray diffractometer. The crystals checked had the same crystallographic features, such as unit cell parameters, and did not show any evidence of nonstoichiometry. The results of the semiquantitative microprobe analysis on several crystals did not show any significant deviation from the composition obtained from the X-ray structure refinements.